

## N-DOPED C/Ti/C/Al/C/Si MULTILAYER AND N-DOPED C+Ti/C+Al/C+Si COMPOSITE THIN FILMS: SYNTHESIS AND CHARACTERIZATION

V. CIUPINA<sup>1,5</sup>, R. VLADOIU<sup>1,5</sup>, G. C. PRODAN<sup>1</sup>, C. POROSNICU<sup>2</sup>, C. LUNGU<sup>2</sup>, V. SATULU<sup>2</sup>,  
A. MANDES<sup>1,\*</sup>, V. DINCA<sup>1</sup>, E. ANDRONESCU<sup>3,5</sup>, B. VASILE<sup>3</sup>, V. NICOLESCU<sup>4</sup>,  
S. POLOSAN<sup>5,6</sup>, E. MATEI<sup>6</sup>

<sup>1</sup> Ovidius University of Constanta, 124 Mamaia Avenue, 900527 Constanta, Romania  
E-mails: vciupina@univ-ovidius.ro; rvladoiu@univ-ovidius.ro; amandes@univ-ovidius.ro;  
vdinca@univ-ovidius.ro; gprodan@univ-ovidius.ro

<sup>2</sup> National Institute for Lasers, Plasma and Radiation Physics, P.O. Box MG-36, 077125 Bucharest, Romania  
E-mails: corneliu.porosnicu@inflpr.ro; anamihair@yahoo.com; veronica.satulu@infim.ro

<sup>3</sup> Universitatea Politehnica Bucuresti, 17 Gh Polizu St, Bucharest 011061, Romania  
E-mails: ec.andronescu@men.edu.ro; vasilebendic@yahoo.com

<sup>4</sup> CERONAV Constanta, Pescarilor Street no. 69A, 900581 Constanta, Romania  
E-mail: virginianicolescu@ceronav.ro

<sup>5</sup> Academy of Romanian Scientists, Ilfov Str. No.3, Bucharest 050094, Romania

<sup>6</sup> National Institute of Materials Physics, 077125, Bucharest-Magurele, Romania  
E-mails: silv@infim.ro; elena.matei@nimp.ro

\* Corresponding author, Email: amandes@univ-ovidius.ro

*Received February 18, 2025*

*Abstract.* The purpose of this work is to obtain different kinds of advanced nanostructures with four materials of interest: carbon, titanium, aluminum and silicon, deposited by Thermionic Vacuum Arc (TVA) technology on the Si substrate, in two cases: C/Ti/C/Al/C/Si multilayer film and C+Ti/C+Al/C+Si composite film with inclusion of nitrogen. Also, for each type of samples some parameters varied: substrates temperature (Room Temperature, 200°C, 300°C, 400°C) and the bias voltage applied on the substrates, *i.e.* – 400 V. Thermal Desorption Spectroscopy (TDS) analyses revealed the presence of nitrogen in all cases. The Raman spectra reveal that the film nitrogen treatments leads to the formation of nitrides for each compound. The infrared absorption spectra are dominated by the formation of C-N bonds, which are the same as in the Raman spectra. EDX and Elemental composition show the values of atomic percentage depending on the substrate deposition temperature. TEM and XPS depth profiles are studied. Based on nanoindentation studies, the Young modulus and hardness are measured. The tribology measurements are also performed.

*Key words:* C/Ti/C/Al/C/Si multilayer, C+Ti/C+Al/C+Si composite, TVA technology, SEM, TEM, EDX, XPS, Raman spectra, Infrared absorption, nanoindentation, tribology measurements.

DOI: <https://doi.org/10.59277/RomRepPhys.2025.77.503>

### 1. INTRODUCTION

Titanium/Aluminum/Silicon-based thin films have a wide range of applications in protective surfaces, machining cutting tools, surface finishing and flexible displays

[1, 2]. To improve the mechanical properties, a successful combination turned out to be the Ti-Si-C-N nanostructures [3–5], CVD and PVD technologies and also the thermospray (plasma spraying) process or plasma-enhanced chemical vapor deposition are used to synthesized such structures. The composition of titanium, silicon, aluminum, carbon, and nitrogen was mixed and deposited using the Thermionic Vacuum Arc (TVA) method to improve the properties of such nanomaterials [6–7]. This method offers convincing advantages for emerging technological applications and provides the possibility of obtaining high-quality structure and tribological properties of different thin films, such as carbon [8–10], tungsten [11], boron [12], carbon-based nanocomposites [13–17], or complex composites [18–20]. The goal was to create different types of nanostructured thin films using four materials of interest: graphite, titanium, silicon, and aluminum, including nitrogen, on the Si substrate, using the TVA method. The structure and properties of the films are highly dependent on the nitrogen content, where non-reactive depositions yield films consisting of  $TiC_x$  [7], Ti, and silicide phases, with a hardness larger than 10 GPa, depending on the nitrogen percentage. Ti-Si-Al-C-N thin films with high contents of Si and C, extend the limits of the two successfully applied ternary systems Ti-Si-N and Ti-C-N in the presence of aluminum. Ti-Si-N thin films generally consist of a few nm sized crystals in an amorphous matrix. The high hardness can be achieved, for example, using 3D nanostructures [21–23]. Several studies have shown that Ti-Si-N coatings exhibit high hardness under optimum deposition conditions, ensuring the complete formation of TiN nanocrystals in the amorphous  $Si_3N_4$  monolayer phase [24–30].

The ternary compounds Ti-C-N, have been intensively investigated because of their mechanical properties. To obtain TiCN coatings with the desired mechanical properties, carbon must be added in a strictly controlled manner [31]. In this respect, the reactive crossed-beam pulsed laser deposition configuration [32], was performed to prepare nanocrystalline thin films of ternary compounds, particularly TiCN compounds [33].

## 2. EXPERIMENTAL RESULTS. DISCUSSIONS

### 2.1. SYNTHESIS OF N-DOPED C/Ti/C/Al/C/Si AND N-DOPED C+Ti/C+Al/C+Si THIN FILMS

The experimental set-up (Fig. 1) is compounded by three plasma sources (anode-cathode) based on C, Al and alternatively on Ti or Si. The deposition was done on the Si substrate at different substrate temperatures (Room Temperature, 200°C, 300°C, 300°C and – 400 V bias voltage, 400°C) resulting in the following samples: Multilayer samples NML<sub>1</sub>, NML<sub>2</sub>, NML<sub>3</sub>, NML<sub>4</sub>, NML<sub>5</sub> (Fig. 2a), and Composite samples NCD<sub>1</sub>, NCD<sub>2</sub>, NCD<sub>3</sub>, NCD<sub>4</sub>, NCD<sub>5</sub> (Fig. 2b) with material thickness presented in Table 1. The Nitrogen flux was maintained at a constant 10 sccm during the deposition process.

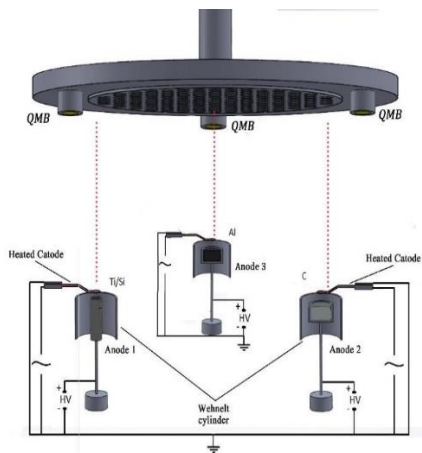


Fig. 1 – The set-up of the TVA technology.

Table 1  
Each material thickness

	Ti, Al, Si Thickness (nm)	Graphite thickness (nm)
Ti + C (100nm)	66	34
Al + C (100nm)	65	35
Si + C (100 nm)	69	31

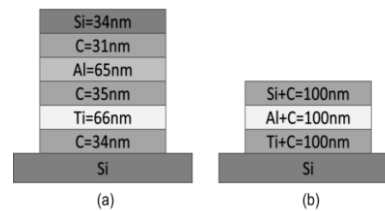


Fig. 2 – Schematic of samples as a function of layers: a) multilayer; b) composite.

## 2.2. CHARACTERIZATION OF C/Ti/C/Al/C/Si MULTILAYER AND C+Ti/C+Al/C+Si COMPOSITE THIN FILMS

### 2.2.1. Thermal desorption spectroscopy (TDS) analysis

The total nitrogen inventory and release from the trapping sites in the composite and multilayer samples were investigated using Thermal Desorption Spectroscopy (TDS). The desorbed species were observed using a QMG 220 Mass spectrometer equipped with a W filament (Fig. 3). The oven was programmed to maintain a stable temperature of 1050°C until the desired gas signal was quenched.

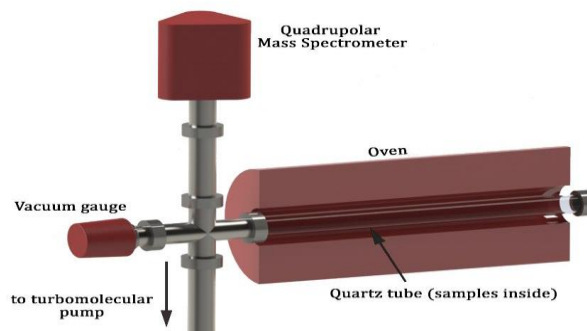


Fig. 3 – TDS set-up.

A comparison between samples NML and NCD, regarding the desorption graphs (atomic nitrogen), in relation to time and temperature, is presented in Fig. 4.

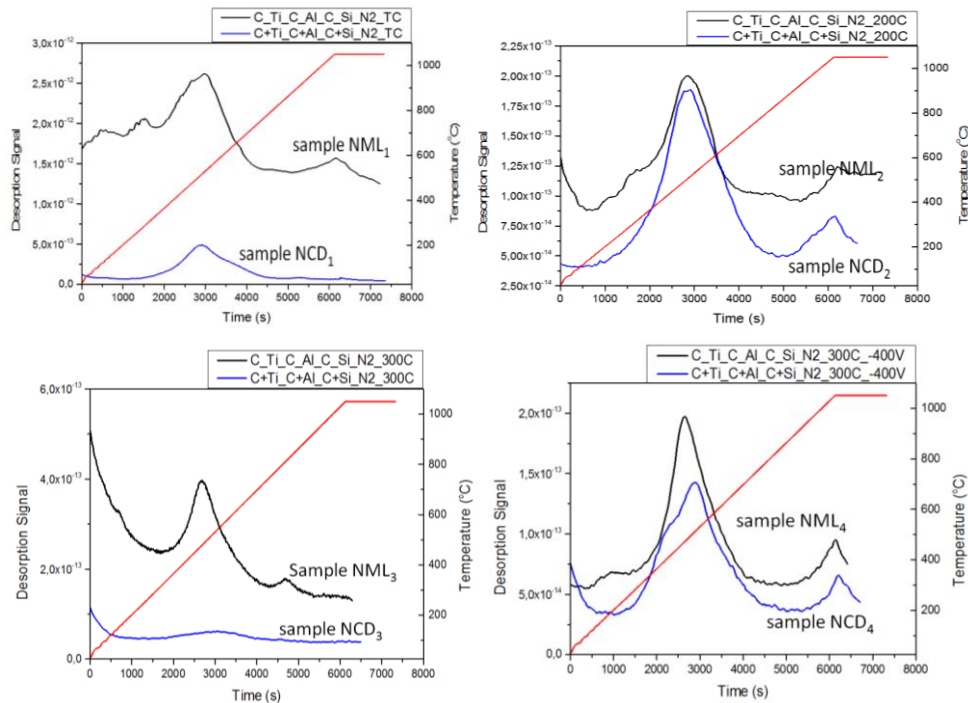


Fig. 4 – Comparison between samples NML and NCD regarding desorption graphs (atomic nitrogen).

Nitrogen desorption maintains the same shape for each sample. There are two desorption peaks, the first desorption starts around 260°C and ends up around 700°C. The second desorption peak is observed at higher temperatures (920°C – 1000°C).

In Fig. 5 are presented the identical desorption spectra presented in Fig. 4, the composite samples and the multilayer samples being plotted on two different graphs.

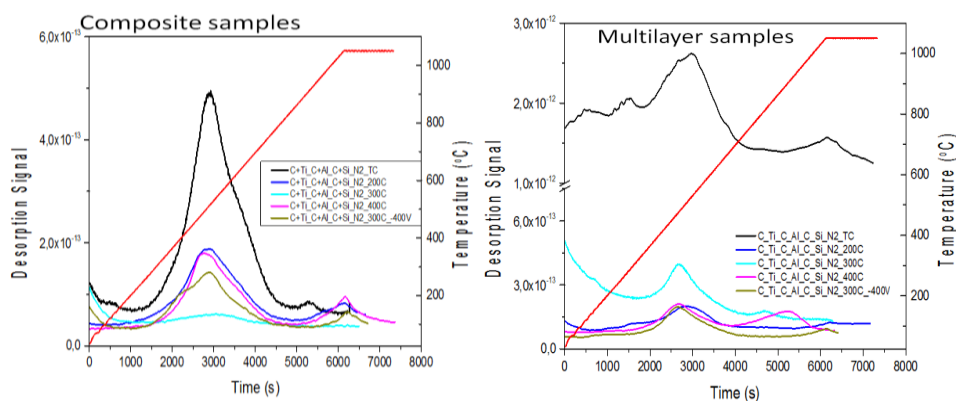


Fig. 5 – Composite samples vs Multilayer samples regarding desorption graphs (atomic Nitrogen).

### 2.2.2. Raman characterization

Nitrogen treatment of the films leads to the formation of nitrides for each compound, *i.e.* aluminum, carbon and silicon nitrides (it should be noted that titanium nitride is similar to aluminum and cannot be differentiated). Thermal treatments of the substrates increased the concentration of nitrides in the films (Fig. 6).

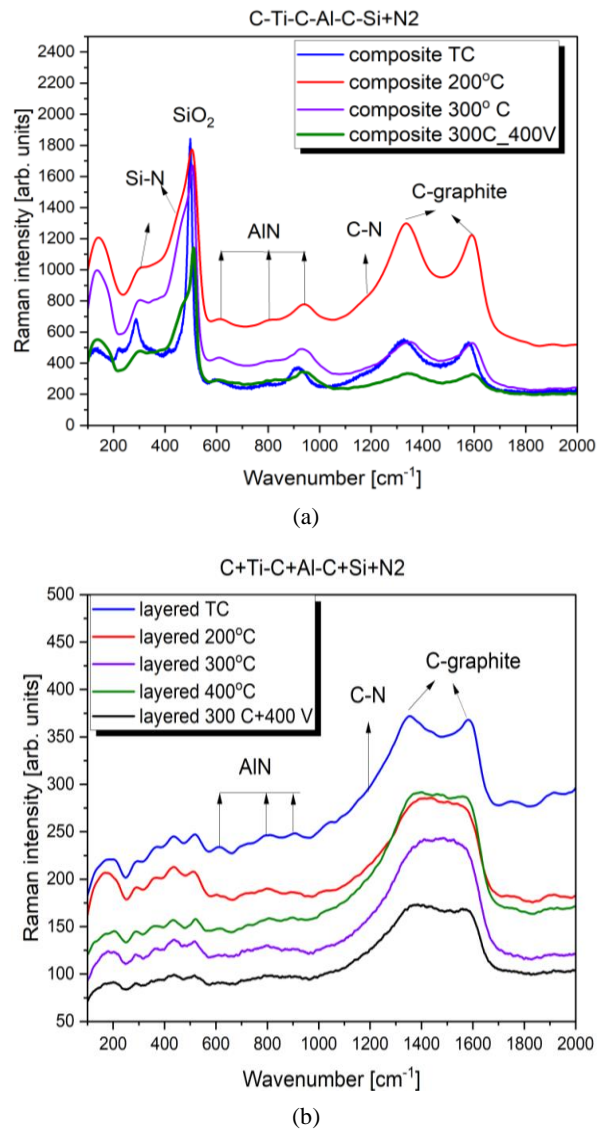


Fig. 6 – Raman spectra: C+Ti/C+Al/C+Si/+N<sub>2</sub> composite samples (a); C/Ti/C/Al/C/Si /+N<sub>2</sub> multilayer samples (b) (Raman excitation 532 nm).

### 2.2.3. Infrared spectroscopy characterization

The infrared absorption spectra (Fig. 7) are dominated by the formation of C-N bonds exactly as in the Raman spectra, whose concentration increases with the increase of the substrate temperature. They are predominant in the layer-type samples where nitration is performed on the carbon layer. Al-N and Si-N vibrations are also observed. In the case of aluminum nitride, heating the substrate leads to a slight increase in the concentration of AlN. More prominent is the increase in Si-N concentration in the sample with substrate heated to 400°C.

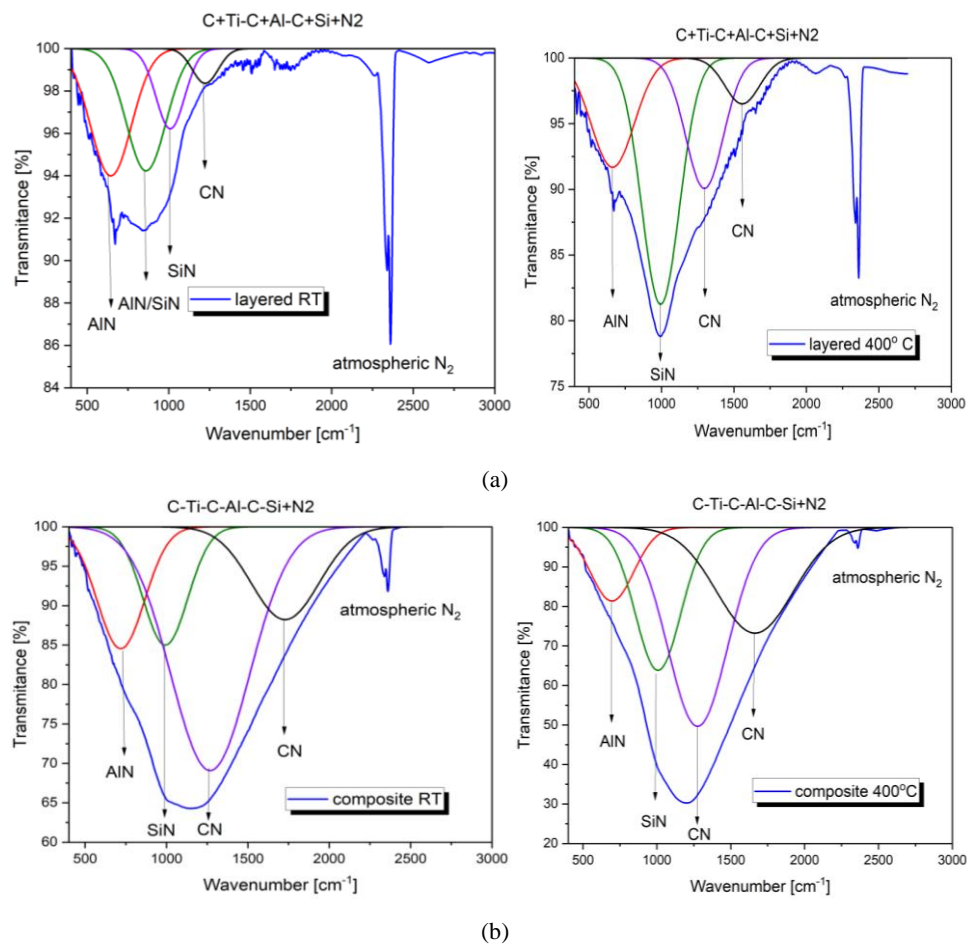


Fig. 7 – Infrared absorption spectra: C/Ti/C/Al/C/Si/+N<sub>2</sub> multilayer samples (a); C+Ti/C+Al/C+Si/+N<sub>2</sub> composite samples (b) in the case of (RT) and at 400°C substrate temperature respectively.

### 2.2.4. TEM analysis

Samples were prepared as XTEM specimens using the Ion Mill techniques. TEM bright field image was used to measure the layers thickness. EDX and STEM mapping were carried out to evaluate the sample composition. In addition, HRTEM images were used for the structural analyze. The sample geometry for sample ML<sub>1</sub> is presented in Fig. 8.

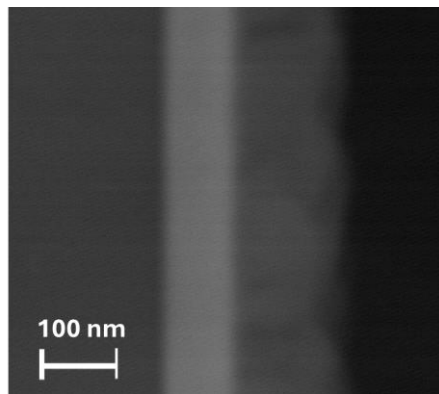


Fig. 8 – Sample geometry for sample ML<sub>1</sub>.

The HRTEM images and corresponding Fourier transforms for the two different zones of sample ML<sub>1</sub> are presented in Fig. 9. We can conclude regarding the structure of the samples that the results prove the polycrystalline character of the Carbon layer and monocrystalline character of the Silicon substrate.

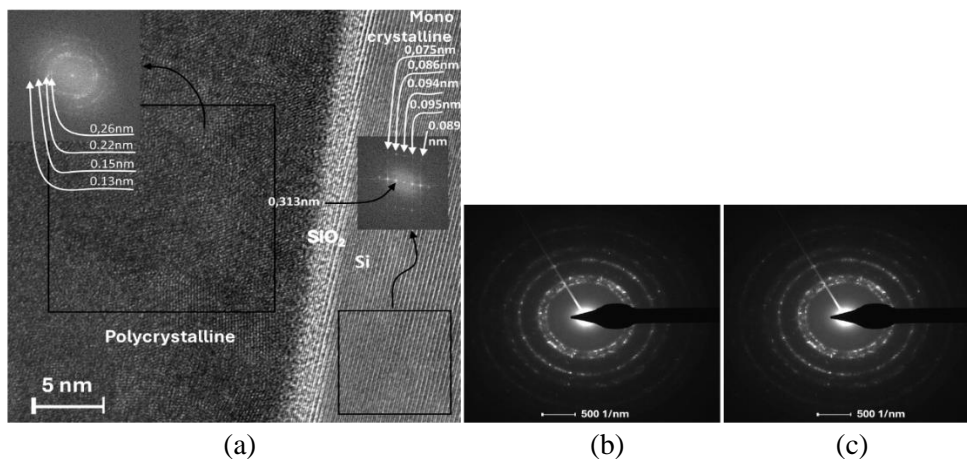


Fig. 9 – HRTEM image and Fourier transform for sample ML<sub>1</sub> (a); diffractograms for: polycrystalline area – Carbon layer (b); monocrystalline area – Silicon substrate (c).

The chemical mapping for sample ML<sub>1</sub> (Fig. 10) shows the presence of elements Al, Si, Ti, C, and also O. Oxygen reacts with silicon resulting in Silicon oxide (SiO<sub>2</sub>) (Fig. 9(a)).

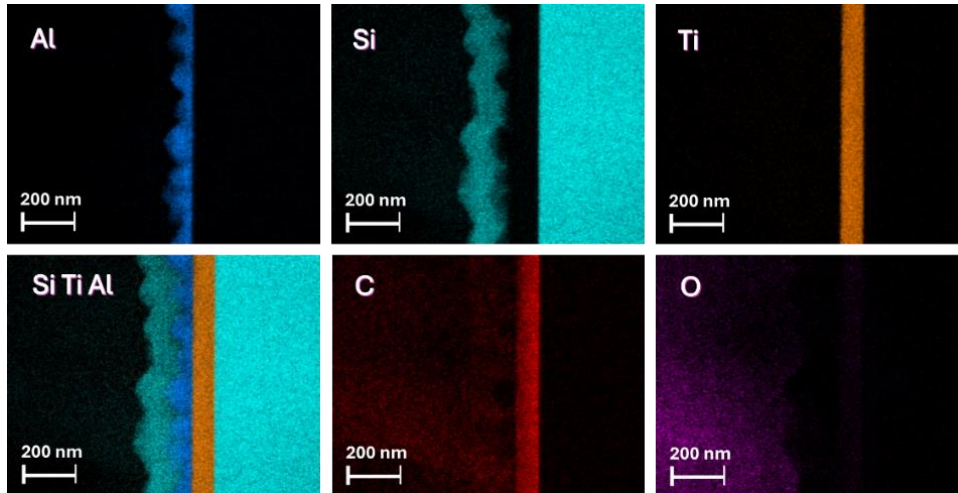


Fig. 10 – Chemical mapping for sample ML<sub>1</sub>.

### 2.2.5. SEM and EDX characterization

The topology of C/Ti/C/Al/C/Si Multilayer films and C+Ti/C+Al/C+Si Composite films, as well as the N-doped C/Ti/C/Al/C/Si and N-doped C+Ti/C+Al/C+Si have been investigated by Scanning Electron Microscopy (SEM) at three magnifications: 1 k $\times$ , 5 k $\times$  and 10 k $\times$ .

In the case of the multilayer films, very smooth surfaces without topological elements were generally observed, as we can see in Fig. 11, at 10 k $\times$  magnification, except in the case of sample CD<sub>4</sub>, when a more pronounced contouring of the grains is observed, due to the – 400 V bias voltage implied in the synthesis of this sample.

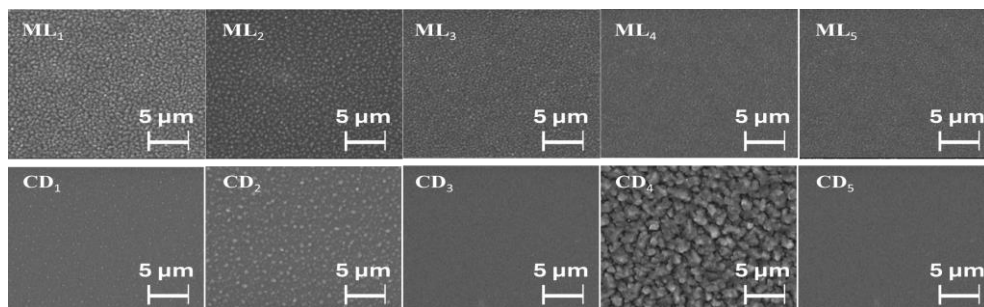


Fig. 11 – The topology of C/Ti/C/Al/C/Si multilayer and C+Ti/C+Al/C+Si composite films (10 k $\times$ ).

The topology of N-doped C/Ti/C/Al/C/Si and N-doped C+Ti/C+Al/C+Si/ thin films is presented in Table 2 and Table 3 respectively, at 1 k $\times$ , 5 k $\times$  and 10 k $\times$  magnification. Generally, very smooth surfaces without topological elements were observed, including in the case of sample CD<sub>4</sub>.

Table 2

The topology of N-doped C/Ti/C/Al/C/Si thin films

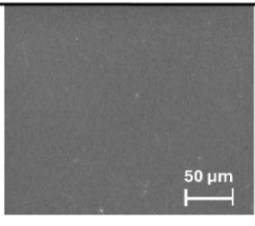
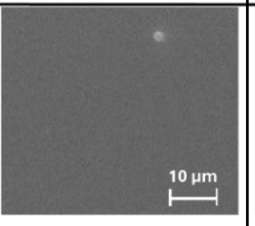
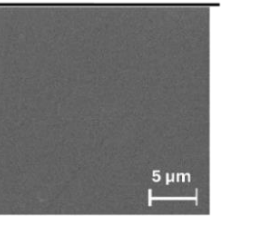
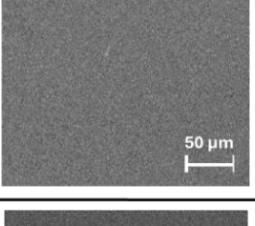
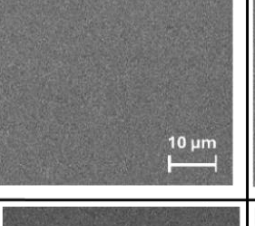
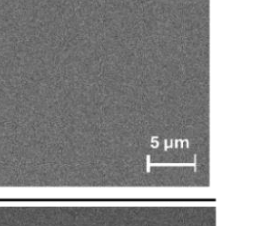
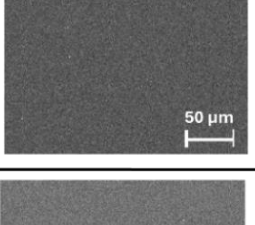
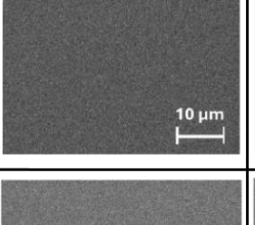
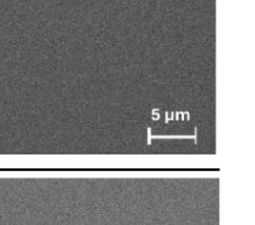
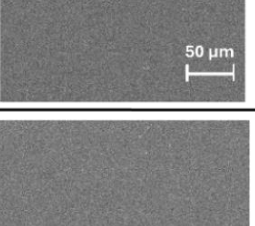
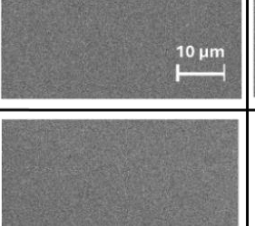
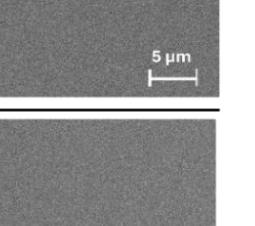
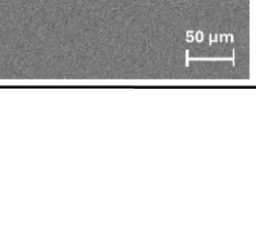
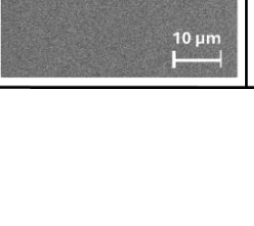
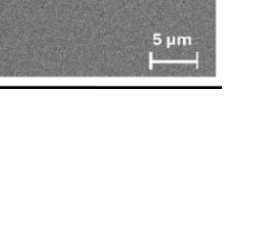
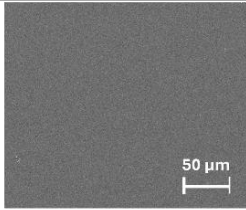
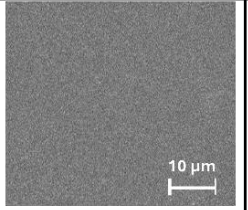
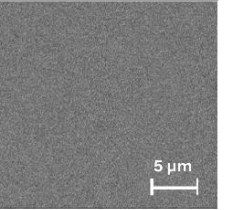
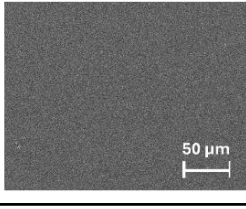
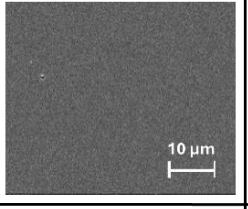
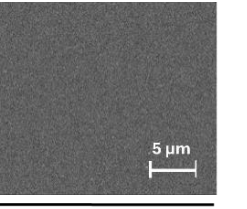
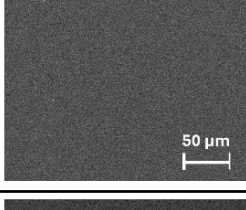
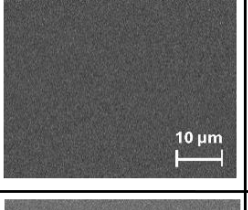
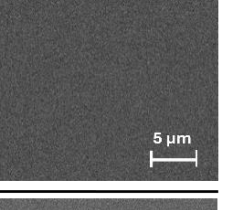
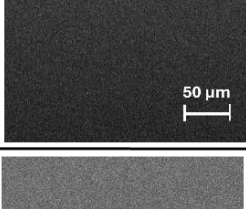
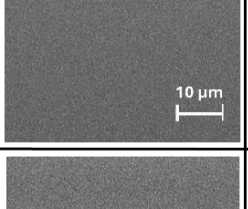
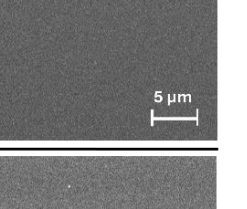
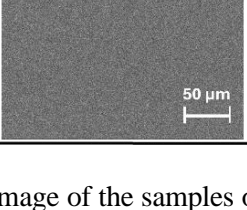
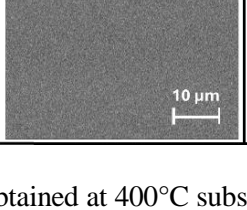
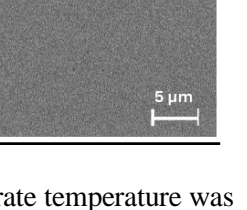
Multilayer (300 nm) N-C/Ti/C/Al/C/Si Temperature	1 kX	5 kX	10 kX
Room Temperature (NML <sub>1</sub> )			
200°C (NML <sub>2</sub> )			
300°C (NML <sub>3</sub> )			
300°C U=-400V (NML <sub>4</sub> )			
400°C (NML <sub>5</sub> )			

Table 3

The topology of N-doped C+Ti/C+Al/C+Si/ thin films

Composite (300 nm) N-C+Ti/C+Al/C+Si Temperature	1 kX	5 kX	10 kX
Room Temperature (NCD <sub>1</sub> )			
200°C (NCD <sub>2</sub> )			
300°C (NCD <sub>3</sub> )			
300°C U=-400V (NCD <sub>4</sub> )			
400°C (NCD <sub>5</sub> )			

The SEM image of the samples obtained at 400°C substrate temperature was examined to observe some phenomena that occurred on the surface of the samples.

Thus, in the case of the N-doped multilayer sample NML<sub>5</sub> (400°C; 3.00 kV; 200.00 k×) (Fig. 12) aggregates of particles can be seen, but they are not crystalline because the diffraction shows an amorphous structure.

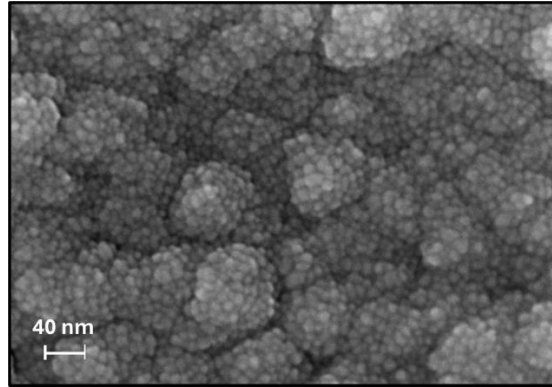


Fig. 12 – Topology of N-doped multilayer sample NML<sub>5</sub> (400°C; 3.00 kV; 200.00 k×).

In the case of the N-doped composite sample NCD<sub>5</sub> (Fig. 13) for: (400°C, 3.00 kV, 150.00 k×) (a); (400°C, 5.00 kV; 100.00 k×) (b); (400°C, 5.00 kV, 200.00 k×) (c), aggregates of particles can be seen with an amorphous structure.

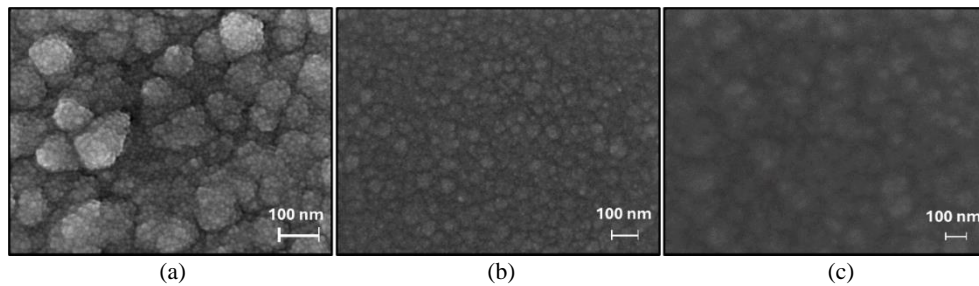


Fig. 13 – Topology of N-doped composite sample NCD<sub>5</sub> for: (400°C, 3.00 kV, 150.00 k×) (a); (400°C, 5.00 kV; 100.00 k×) (b); (400°C, 5.00 kV, 200.00 k×) (c).

### 2.2.6. EDX spectra. Elemental composition characterisation: C+Ti/C+Al/C+Si composite thin films at different deposition temperatures

The atomic % of O, Al, Si, and Ti obtained from the EDX spectra for the C/Ti/C/Al/C/Si Multilayer and C+Ti/C+Al/C+Si Composite samples are presented in Fig. 14. It can be observed that Atomic % of O, Al, Si, and Ti register significant changes depending on the deposition temperature for the two types of samples. Thus, for example, in the case of sample CD<sub>3</sub> (300°C), compared with the sample CD<sub>4</sub> (300°C; – 400 V) (+) the Si2p percent decreased from 72.93% to 58.16% and also the O1s percent decreased from 16.04% to 13.11% as a result of the application of the – 400 V bias voltage, the deposited temperature remaining the same. It should be mentioned that nitrogen is missing in the presented spectra (the spectra of samples undoped with nitrogen).

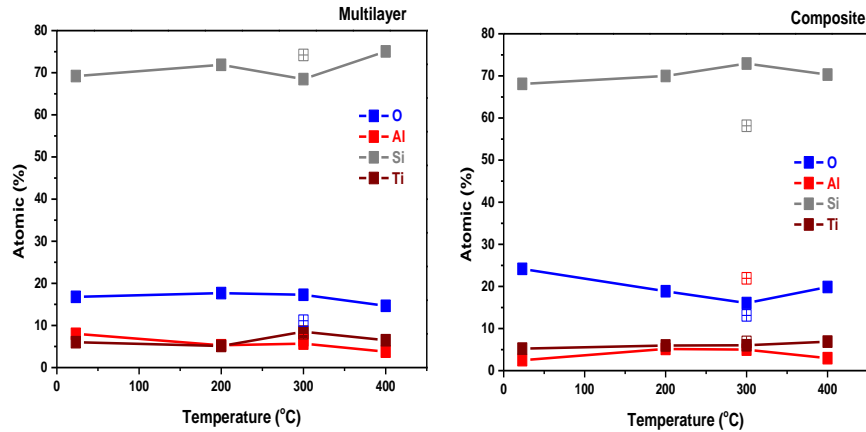


Fig. 14 – Atomic % of O, Al, Si, and Ti obtained from EDX spectra for C/Ti/C/Al/C/Si multilayer and C+Ti/C+Al/C+Si composite samples.

The EDX measured spectra in the case of N doped-multilayer samples (C/Ti/C/Al/C/Si/+N<sub>2</sub>) and N doped-composite samples (C+Ti/C+Al/C+Si/+N<sub>2</sub>) respectively, are presented as follows:

In the case of the N- doped-multilayer samples (C/Ti/C/Al/C/Si/+N<sub>2</sub>) (Fig. 15), first of all, it should be mentioned that nitrogen is present in these spectra (that is, the spectra of samples doped with nitrogen). Also, as can be seen from the data, we cannot discern how much silicon we have because it is also the influence of the substrate. Also, a maximum appears at 0.88 keV, may due of: neon (gas), nickel, lantana or cerium.

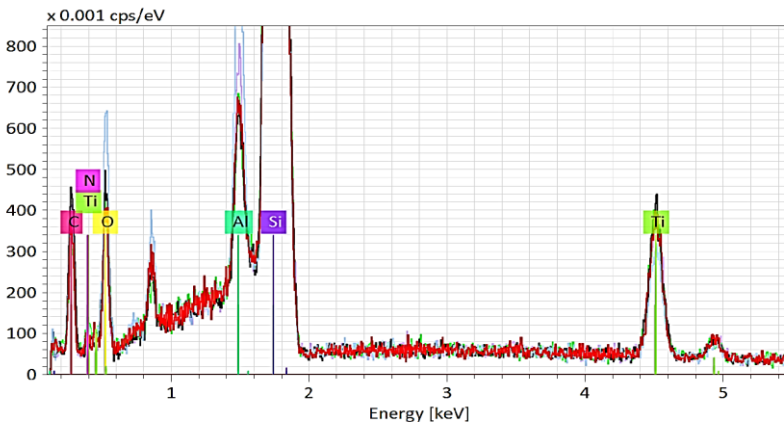


Fig. 15 – EDX spectra in the case of N doped-multilayer samples (C/Ti/C/Al/C/Si/+N<sub>2</sub>).

In the case of N-doped composite samples (C+Ti/C+Al/C+Si/+N<sub>2</sub>) (Fig. 16), it should be mentioned that nitrogen is present in spectra of composite samples

doped with nitrogen. Also, like in the previous case, is not possible to discern from the data how much silicon we have because of the influence of the substrate. We suppose that maximum from 0.88 keV, possibly due to the elements: neon (gas), nickel, lantana or cerium.

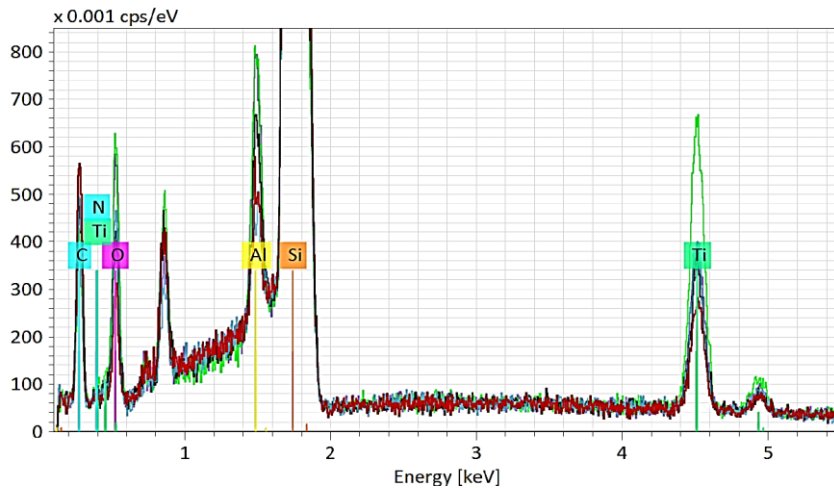


Fig. 16 – EDX spectra in the case of N doped-composite samples (C+Ti/C+Al/C+Si/+N<sub>2</sub>).

To reduce the influence of the substrate we attempted measurements at different acceleration voltages (Tables 4, 5, and 6). These tables include the average density of the films and the penetration depth for each applied voltage; the colors in the tables are those in the graphs of the EDX spectra presented previously for the N-doped samples.

Table 4

20 kV acceleration voltage

Method	Sample	Density (g/cm <sup>3</sup> )	Penetration (μm)	Color on previous graphs
Multilayer	TC	2.18	3.5	mauve
	200°C	2.15	3.6	green
	300°C	2.17	3.5	black
	400°C	2.10	3.6	blue
	300°C – 400 V	2.17	3.6	red
Composite	TC	2.13	3.6	mauve
	200°C	2.14	3.6	green
	300°C	2.18	3.5	black
	400°C	2.18	3.5	blue
	300°C, – 400 V	2.21	3.5	red

Table 5

10 kV acceleration voltage

Method	Sample	Density (g/cm <sup>3</sup> )	Penetration (μm)	Color on previous graphs
Multilayer	TC	2.34	1.1	mauve

Table 6

5 kV acceleration voltage

Method	Sample	Density (g/cm <sup>3</sup> )	Penetration (μm)	Color on previous graphs
Multilayer	TC	2.24	0.3	mauve

The penetration depth decreases to 300 nm at 5 kV, but Ti is no longer visible, because the sensitivity also decreases.

### 2.2.7. XPS analyses

XPS analyses were performed on a K-Alpha Thermo Scientific (ESCALAB™ XI+, East Grinstead, UK) spectrometer equipped with a 180° double-focusing hemispherical analyzer.

XPS depth-profiles are represented from the left (position 0 on the X-axis representing the surface of the film) to the right to the substrate.

In the case of composite samples, the results of the studies are presented in Figs. 17 and 18.

Figure 17 shows the XPS result for the composite sample deposited at room temperature (CD<sub>1</sub>). The oxygen is present at the thin film surface, then decreases with respect to the sample depth; however, it has a peak around 4000 seconds, probably due to the chemical affinity with the two elements Ti and Al respectively. For Si, a clear behavior is distinguished. It is present in the first layer, as desired. Then, at the end of the spectra, an abrupt increase of the Si concentration determined by the substrate was observed. Further analysis of the XPS spectrum, revealed that a broadened peak of Al is differentiated, between 1000 s and 3000 s, followed by the one for Ti, the very first layer deposited on top of the Si substrate.

Figure 18 shows the XPS spectrum for the composite sample prepared at of 300°C and – 400 V bias voltage (CD<sub>4</sub>). The peaks of the three materials Si, Al and Ti are well defined. The O concentration is much lower, due to the high working temperature. However, we observed a broadening of the Al peak that starts at 800 s and continues above the value of 5000 s.

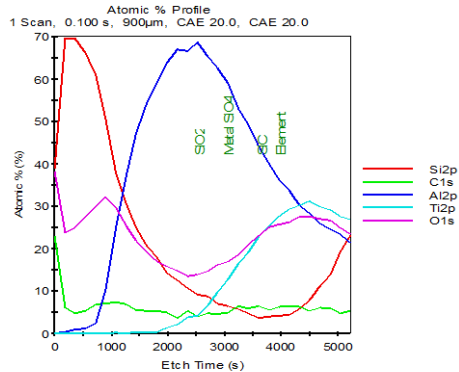


Fig. 17 – XPS result for the composite sample CD<sub>1</sub>.

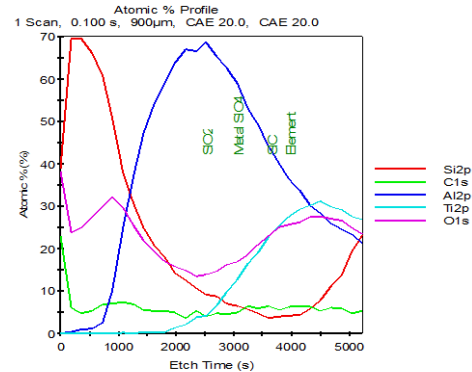
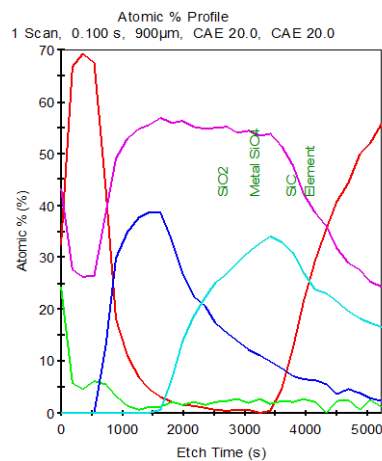
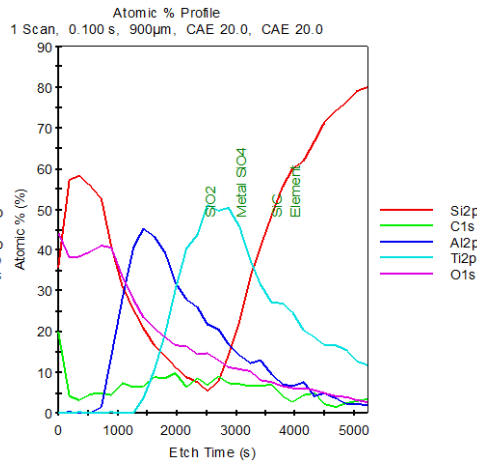


Fig. 18 – XPS spectrum for the composite sample CD<sub>4</sub>.

The results of the studies are presented in Fig. 19 for the multilayer films (C/Ti/C/Al/C/Si) prepared at room temperature (ML<sub>1</sub>) (a) and at a temperature of 300°C and a bias voltage of –400 V (ML<sub>4</sub>) (b).



(a)



(b)

Fig. 19 – XPS spectra for multilayer films (C/Ti/C/Al/C/Si) prepared at room temperature (ML<sub>1</sub>) (a) and at temperature of 300°C and bias voltage of –400 V (ML<sub>4</sub>) (b).

The oxygen concentration gives a clear difference between the two graphs. For the sample deposited at room temperature (ML<sub>1</sub>) (a), the O concentration is increased and present throughout the thickness of the sample. The oxygen concentration decreased along the sample depth in the second sample (ML<sub>4</sub>) (b). For both spectra, the peaks of the three materials (Si, Al, Ti) used are well-defined and each thickness can be calculated separately. For the Ti peaks, a slight increase

can be observed in case of the ML<sub>4</sub> sample, but we cannot conclude that it is due to the working conditions.

### 2.2.8. Nanoindentation characterization

The investigation was carried out with the help of a Bruker nanoindenter. Quantitative force measurements allow the system to extrapolate mechanical properties such as the Elastic modulus, Hardness, Coefficient of friction and Wear resistance.

**Nanoindentation.** Results for C/Ti/C/Al/C/Si Multilayer films and C+Ti/C+Al/C+Si Composite films with a partial unload function (2000  $\mu$ N) and the Basic QS Trapezoid are presented in Table 7.

Table 7

Values of Young modulus and hardness in the two Load function  
(Partial Unload and Basic QS Trapezoid)

Sample	Load function	
	Partial Unload	Basic QS Trapezoid
C/Ti/C/Al/C/Si (ML <sub>1</sub> ) (Room temperature)	Young Modulus: 107.70 GPa Hardness: 2.15 GPa	Young Modulus: 92.87 GPa Hardness: 1.81 GPa
C+Ti/C+Al/C+Si (CD <sub>1</sub> ) (Room temperature)	Young Modulus: 82.22 GPa Hardness: 6.82 GPa	Young Modulus: 72.65 GPa Hardness: 6.65 GPa
C/Ti/C/Al/C/Si (ML <sub>2</sub> ) (200°C)	Young Modulus: 37.90 GPa Hardness: 1.19 GPa	–
C+Ti/C+Al/C+Si (CD <sub>2</sub> ) (200°C)	–	Young Modulus: 71.65 GPa Hardness: 3.32 GPa
C/Ti/C/Al/C/Si (ML <sub>3</sub> ) (300°C)	Young Modulus: 83.82 GPa Hardness: 2.90 GPa	Young Modulus: 79.32 GPa Hardness: 2.63 GPa
C+Ti/C+Al/C+Si (CD <sub>3</sub> ) (300°C)	Young Modulus: 75.52 GPa Hardness: 2.62 GPa	Young Modulus: 85.63 GPa Hardness: 3.28 GPa
C/Ti/C/Al/C/Si (ML <sub>5</sub> ) (400°C)	Young Modulus: 79.13 GPa Hardness: 3.09 GPa	Young Modulus: 64.28 GPa Hardness: 1.83 GPa
C+Ti/C+Al/C+Si (CD <sub>5</sub> ) (400°C)	Young Modulus: 68.38 GPa Hardness: 2.46 GPa	Young Modulus: 71.98 GPa Hardness: 2.60 GPa
C/Ti/C/Al/C/Si (ML <sub>4</sub> ) (300°C; –400 V)	Young Modulus: 107.07 GPa Hardness: 5.54 GPa	Young Modulus: 118.83 GPa Hardness: 6.98 GPa
C+Ti/C+Al/C+Si (CD <sub>4</sub> ) (300°C; –400 V)	Young Modulus: 76.09 GPa Hardness: 2.58 GPa	Young Modulus: 78.70 GPa Hardness: 2.57 GPa C/Ti/C/Al/C/Si (T 300°C; –400 V)

Tables 8 and 9 show the nanoindentation results obtained for the N-doped Composite and Multilayer samples respectively.

Table 8

Young modulus and hardness for N-doped composite samples

Sample	Load Function	
	Partial Unload	Basic QS Trapezoid
N-C+Ti/C+Al/C+Si (NCD <sub>1</sub> ) (Room temperature)	Young Modulus: 91.19 GPa Hardness: 8.66 GPa	Young Modulus: 86.08 GPa Hardness: 8.77 GPa
N-C+Ti/C+Al/C+Si (NCD <sub>2</sub> ) (200°C)	Young Modulus: 83.12 GPa Hardness: 7.82 GPa	Young Modulus: 72.63 GPa Hardness: 7.62 GPa
N-C+Ti/C+Al/C+Si (NCD <sub>3</sub> ) (300°C)	Young Modulus: 80.15 GPa Hardness: 9.33 GPa	Young Modulus: 72.86 GPa Hardness: 8.74 GPa
N-C+Ti/C+Al/C+Si (NCD <sub>5</sub> ) (400°C)	Young Modulus: 79.80 GPa Hardness: 7.95 GPa	Young Modulus: – GPa Hardness: – GPa
N-C+Ti/C+Al/C+Si (NCD <sub>4</sub> ) (300°C; –400 V)	Young Modulus: 25.55 GPa Hardness: 3.70 GPa	Young Modulus: 16.30 GPa Hardness: 3.80 GPa

Table 9

Young modulus and hardness for N-doped multilayer samples

Sample	Load Function	
	Partial Unload	Basic QS Trapezoid
N-C/Ti/C/Al/C/Si (NML <sub>1</sub> ) (Room temperature)	Young Modulus: 80.52 GPa Hardness: 7.13 GPa	Young Modulus: 78.42 GPa Hardness: 7.26 GPa
N-C/Ti/C/Al/C/Si (NML <sub>2</sub> ) (200°C)	Young Modulus: 37.10 GPa Hardness: 5.16 GPa	Young Modulus: 28.09 GPa Hardness: 4.97 GPa
N-C/Ti/C/Al/C/Si (NML <sub>3</sub> ) (300°C)	Young Modulus: 65.64 GPa Hardness: 5.53 GPa	Young Modulus: 65.43 GPa Hardness: 5.35 GPa
N-C/Ti/C/Al/C/Si (NML <sub>5</sub> ) (400°C)	Young Modulus: 57.13 GPa Hardness: 4.37 GPa	Young Modulus: 57.89 GPa Hardness: 4.71 GPa
N-C/Ti/C/Al/C/Si (NML <sub>4</sub> ) (300°C; –400 V)	Young Modulus: 48.50 GPa Hardness: 4.73 GPa	Young Modulus: 41.95 GPa Hardness: 4.73 GPa

Taking into account Tables 7, 8 and 9, we can compare the values of the Hardness, as seen below, for multilayer films (a) and composite films (b) in the cases of samples synthesized at Room Temperature (RT), 200°C, 300°C, 300°C and –400 V, 400°C (the values in GPa, for undoped samples and doped samples in parentheses).

(a) C/Ti/C/Al/C/Si (N-doped C/Ti/C/Al/C/Si) multilayer films

RT: 2.15 (7.13); 200°C: 1.19 (5.16); 300°C: 2.90 (5.53); 300°C and –400 V: 5.54 (4.73); 400°C: 3.09 (4.37).

(b) C+Ti/C+Al/C+Si (N-doped C+Ti/C+Al/C+Si) composite

RT: 6.82 (8.66); 200°C: – (7.82); 300°C: 2.62 (9.33); 300°C and –400 V: 2.58 (3.70); 400°C: 2.46 (7.95).

The data reveal that the values of the Hardness in the case of the N-doped thin films are generally bigger compared with the values in the case of undoped samples (especially in the case of composite samples).

### 2.2.9. Tribology characterisation

The study was carried out by using a CSM Switzerland ball Tribometer under normal pressure and humidity conditions by counter-friction of thin layers by a stainless steel ball placed in the head of the measuring arm of the tribometer. The tribology measurements normal loading forces were 0.5 N, 1 N, 2 N and 3 N, respectively, over a sliding distance of 30 m with a linear speed of 2 cm/s. For tribology measurements the normal loading forces used were 0.5 N, 1 N, 2 N and 3 N, respectively. The measurements show that the friction coefficient increased with the load force. For example, Figs. 20 and 21 present the friction coefficient vs. the sliding distance in the samples  $ML_1$ ,  $NML_1$ ,  $CD_1$  and  $NCD_1$ .

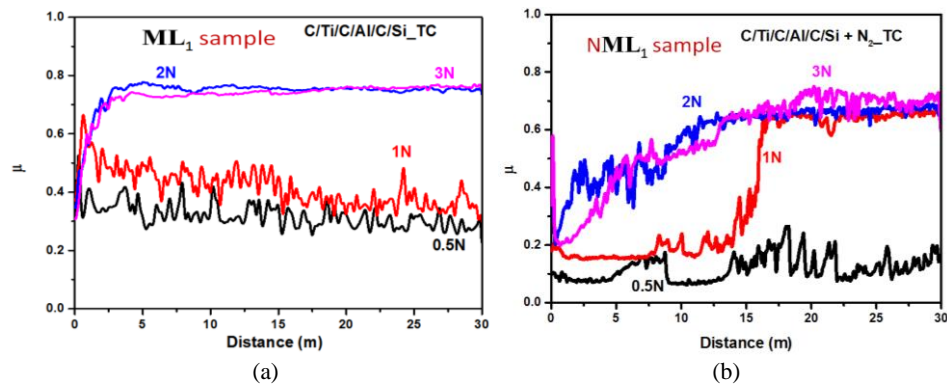


Fig. 20 – (a) Friction coefficient increase with increase of load: from 0.35 at 0.5 N to 0.75 at 3 N; (b) friction coefficient increase with increase of load: from 0.04 at 0.5 N to 0.65 at 3 N.

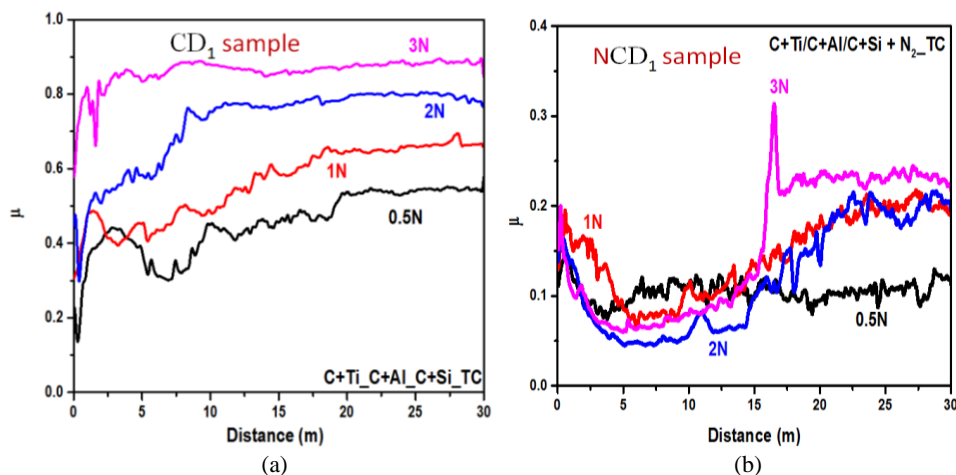


Fig. 21 – (a) Friction coefficient increase with increase of load: from 0.45 at 0.5 N to 0.9 at 3 N; (b) friction coefficient increase with increase of load: from 0.1 at 0.5 N to 0.25 at 3 N.

For comparison, the friction coefficient values are presented in Table 10: values of minimum at 0.5 N load (maximum at 3 N load) at different deposition temperatures.

Table 10

A comparison view of the friction coefficient values

Deposition temperature	C/Ti/C/Al/C/Si multilayer	N-doped C/Ti/C/Al/C/Si multilayer
RT	0.35 (0.04)	0.50 (0.65)
200°C	0.42 (0.25)	0.75 (0.65)
300°C	0.25 (0.35)	0.83 (0.75)
300°C; -400 V	0.32 (0.20)	0.87 (0.55)
400°C	0.25 (0.39)	0.79-at 2 N load (0.75)

Deposition temperature	C+Ti/C+Al/C+Si composite	N-doped C+Ti/C+Al/C+Si composite
RT	0.45 (0.10)	0.90 (0.25)
200°C	0.57 (0.05)	0.83 (0.43)
300°C	0.58 (0.09)	0.78 (0.013)
300°C; -400 V	0.58 (0.02)	0.78 (0.15-at 2 N load)
400°C	0.45 (0.12)	0.89 (0.18)

The data reveal that the friction coefficient values in the case of the N-doped thin films are generally smaller than those in the undoped samples (especially in the case of composite samples) concerning the growth of hardness. We suppose the measured values of the friction coefficient are associated with the occurrence of the atomic diffusion process at the interfaces.

### 3. CONCLUSIONS

C, Ti, Al and Si, including nitrogen, were deposited on the Si substrates by the TVA technology using three independent anode-cathode plasma sources. The final thickness of the C/Ti/C/Al/C/Si Multilayer and C+Ti/C+Al/C+Si Composite thin films, thus obtained, was 300 nm. Also, varied substrate temperatures (room temperature, 200°C, 300°C, 400°C) and bias voltage were applied to the substrates (-400 V) for each sample type.

Thermal desorption analysis revealed that the nitrogen desorption retained the same shape for each sample, despite the deposition conditions used. The same nitrogen release behaviour was observed in all the cases given by two desorption peaks; the first desorption started around 260°C and ended up around 700°C. The second desorption peak is observed at higher temperatures (920°C -1000°C).

SEM, STEM, HRTEM and EDX characterizations of the C/Ti/C/Al/C/Si Multilayer thin films and the C+Ti/C+Al/C+Si Composite thin films were

performed. The EDX measured spectra in the case of N-doped multilayer samples (C/Ti/C/Al/C/Si/+N<sub>2</sub>) and N-doped composite samples (C+Ti/C+Al/C+Si/+N<sub>2</sub>) reveal, in all cases, the presence of nitrogen.

The elemental composition of the C/Ti/C/Al/C/Si Multilayer thin films and C+Ti/C+Al/C+Si Composite thin films are presented at different deposition substrate temperatures. It can be observed that the atomic % of O, Al, Si, and Ti register significant changes depending on the deposition temperature for the two types of samples.

The Raman spectra reveal that the nitrogen treatment of the films leads to the formation of nitrides for each compound, *i.e.* aluminum, carbon and silicon nitrides. Thermal treatment of the substrates increased the concentration of nitrides in the films. However, they generally do not have a well-defined crystallographic structure, being more quickly an agglomeration of particles.

The infrared absorption spectra are dominated by the formation of C-N bonds exactly as in the Raman spectra, whose concentration increases with the increase of the substrate temperature. They are predominant in the layer-type samples where nitriding is performed on the carbon layer. Al-N and Si-N vibrations are also observed. In the case of aluminum nitride, heating the substrate leads to a slight increase in the concentration of AlN. More prominent is the increase in the Si-N concentration in the substrate heated to 400°C.

Based on the nanoindentation measurements, the Young's modulus and hardness for the C/Ti/C/Al/C/Si multilayer thin films, C+Ti/C+Al/C+Si composite thin films, N-C/Ti/C/Al/C/Si multilayer thin films, and N-C+Ti/C+Al/C+Si composite thin films are presented. The data obtained reveal that the hardness values for the doped thin films are generally higher than those for the undoped samples (especially in the case of composite samples).

The tribology data reveal that the values of the friction coefficient in the case of N-doped thin films are generally smaller compared with the values in the case of undoped samples (especially in the case of composite samples), concerning the growth of hardness. The measured values of the friction coefficient are associated with the occurrence of the atomic diffusion process at the interfaces.

#### REFERENCES

1. C. Ciobotaru, M. Enculescu, S. Polosan, I. Enculescu and C. C. Ciobotaru, *Micromachines* **14**, 543 (2023).
2. B.I. C. Ciobotaru, S. Polosan, M. Enculescu, A. Nitescu, I. Enculescu, M. Beregoi, C. C. Ciobotaru, *Nanotechnology* **33**, 395203 (2022).
3. D.-H. Kuo, K.-W. Huang, *Surf Coat Tech.* **202**, 915 (2007).
4. D.-H. Kuo, K.-W. Huang, *Thin Solid Films* **394**, 72 (2001).
5. D.-H. Kuo, W.-C. Liao, *Thin Solid Films* **394**, 81 (2001).
6. V. Ciupina, R. Vladioiu, C. Lungu, V. Dinca, M. Contulov, A. Mandes, P. Popov, G. Prodan, *EPJ D* **66**, 99 (2012).

7. V. Ciupina, C. P. Lungu, R. Vlădoiu, *et al.*, *Physica Scripta* **95**, 044012 (2020).
8. G. Musa, I. Mustata, M. Blideran V. Ciupina, R. Vlădoiu, G. Prodan, E. Vasile, H Ehrich, *Acta Physica Slovaca* **55**, 417–421 (2005).
9. R. Vlădoiu, V. Dinca, G. Musa, *Eur. Phys. J. D* **54**, 433–437 (2009).
10. G. Musa, R. Vlădoiu, V. Ciupina, J. Janik, *J. Optoelectron. Adv. Mater.* **8**, 1617–1620 (2006).
11. R. Vlădoiu, V. Ciupina, C.P. Lungu, V. Bursikova, G. Musa, *J. Optoelectron. Adv. M.* **8**, 71–73 (2006).
12. T. Akan, N. Ekem, S. Pat, U.G. Issever, M.Z. Balbag, M.I. Cenik, R. Vlădoiu, G. Musa, *Mater. Lett.* **61**, 23–26 (2007).
13. R. Vlădoiu, A. Mandes, V.D. Balan, G. Prodan, V. Ciupina, *Rom. Rep. Phys.* **68**, 1076–1084 (2016).
14. A. Mandes, R. Vlădoiu, V. Dinca, G. Prodan, *IEEE Transactions on Plasma Science* **42**, 2806–2807 (2014).
15. R. Vlădoiu, V. Ciupina, A. Mandes, M. Contulov, V. Dinca, P. Popov, C.P. Lungu, *Rom. Rep. Phys.* **63**, 1053–1060 (2011).
16. R. Vlădoiu, V. Ciupina, M. Contulov, A. Mandes, V. Dinca, G. Prodan, C.P. Lungu, *J. Opt. Adv. Mater.* **12**, 553–556 (2010).
17. V. Ciupina, R. Vlădoiu, A. Mandes, G. Musa, C. P. Lungu, *J. Opt. Adv. Mater.* **10**, 2958–2962 (2008).
18. R. Vlădoiu, A Mandes, V. Dinca, P. Kudrna, M. Tichý, S.Polosan, *J. Alloys & Comp.* **869**, 159364 (2021).
19. V. Dinca, A. Mandes, R. Vlădoiu, G. Prodan, V. Ciupina, S. Polosan, *Coatings* **13**, 13060984 (2023).
20. R. Vlădoiu, A. Mandes, V. Dinca, E. Matei, S. Polosan, *Coatings* **12**(4) (2022).
21. S. Veprek, S. Reiprich, *Thin Solid Films* **268**, 64 (1995).
22. A.A. Voevodin, J.S. Zabinski, *Thin Solid Films* **370**, 223 (2000).
23. P.H. Mayrhofer, C. Mitterer, J.G. Wen, J.E. Greene, I. Petrov, *Appl. Phys. Lett.* **86**, 131909 (2005).
24. S. Veprek, S. Reiprich, L. Shizhi, *Appl. Phys. Lett.* **66**, 2640 (1995).
25. S. Veprek, A. Niederhofer, K. Moto, T. Bolom, H.-D. Männling, P. Nesladek, G. Dollinger, A. Bergmaier, *Surf. Coat. Technol.* **152**, 133–134 (2000).
26. S. Veprek, A.S. Argon, *J. Vac. Sci. Technol. B* **20**, 650 (2002).
27. S. Veprek, *Thin Solid Films* **317**, 449 (1998).
28. A. Niederhofer, T. Bolom, P. Nesladek, K. Moto, C. Eggs, D.S. Patil, S. Veprek, *Surf. Coat. Technol.* **183**, 146–147 (2001).
29. S. Veprek, M.G.J. Veprek-Heijman, P. Karvankova, J. Prochazka, *Thin Solid Films* **476**, 1 (2005).
30. R.F. Zhang, A.S. Argon, S. Veprek, *Phys. Rev. B* **81**, 245418 (2010).
31. R. Hauert, J. Patscheider, *Adv. Eng. Mater.* **2**, 247 (2000).
32. L. Escobar-Alarcón, E. Camps, S. Romero, S. Muhl, I. Camps, E. Haro-Poniatowski, *Appl. Phys. A: Mater. Sci. Process.* **101**, 771 (2010).
33. C.C. Chen, N.T. Liang, W.S. Tse, I.Y. Chen, J.D. Duh, *Chin. J. Phys.* **32**, 205 (1994).